submitted to QCPE.
(17) For a summary of available data see ref 12.
(18) The small effects observed here are consistent with the magnitudes of rotational barriers calculated[19] and observed[11] for β-substituted ethyl radicals.
(10) L. Radom, J. Paviot, J. A. Pople, and P. v. R. Schleyer, *J. Chem. Soc., Chem. Commun.*, 58 (1974).
(20) (a) V. J. Shiner, B. L. Murr, and G. Heinemann, *J. Am. Chem. Soc.*, **85**, 2413 (1963); (b) M. Tarle, S. Borčić, and D. E. Sunko, *J. Org. Chem.*, **40**, 2049 (1975). The origin of inductive isotope effects is not clear. See E. K. Thornton and E. R. Thornton, *ACS Monogr.*, **No. 167**, 000 (1970).

(21) (a) N. C. Evans and G. Y. S. Lo, *J. Am. Chem. Soc.*, **88**, 2118 (1966); (b) G. A. Olah, E. B. Baker, J. C. Evans, W. S. Tolgyesi, J. S. McIntyre, and I. J. Bastien, *ibid.*, **86**, 1360 (1964); (c) G. A. Olah, A. Commeyras, J. DeMember, and J. L. Bribes, *ibid.*, **93**, 459 (1971).
(22) See, for example, L. Radom, W. J. Hehre, and J. A. Pople, *J. Am. Chem. Soc.*, **94**, 2371 (1972), and references cited therein.
(23) For a recent discussion of the geometrical structures of X–CH₂⁻ systems see A. Prose, D. J. DeFrees, B. A. Levi, S. K. Pollack, L. Radom, and W. J. Hehre, *J. Am. Chem. Soc.*, to be submitted.
(24) It should be noted that the actual (4-31G level) equilibrium structure for the ethyl anion incorporates a nearly tetrahedral carbanion center.

Oxygen-17 Nuclear Quadrupole Double Resonance Spectroscopy. 1. Introduction. Results for Organic Carbonyl Compounds[1]

C. P. Cheng and Theodore L. Brown*

Contribution from the School of Chemical Sciences, University of Illinois—Urbana, Urbana, Illinois 61801. Received October 6, 1978

Abstract: The pure nuclear quadrupole resonance (NQR) spectra of [17]O in natural abundance in 23 substances containing carbonyl groups are reported. The spectra were obtained on powdered solids at 77 K, using the double resonance field cycling technique pioneered by Hahn and co-workers. The substances studied include $C_6H_5C(O)X$ (X = F, Cl, Br, CN), substituted benzaldehydes, phenyl benzoate, several acid anhydrides, phthalimide, $KHCO_3$, $NaHCO_3$, sodium formate, and potassium acid phthalate. An analysis of the carbonyl oxygen data in terms of a simple Townes–Dailey model shows that variation in carbon–oxygen π bond character among the compounds is the major source of variations in quadrupole coupling constant and asymmetry parameter. The atomic orbital populations on oxygen deduced from the NQR data are in accord with the limited physical data and theoretical results available for comparisons.

Introduction

Oxygen-17, the sole isotope of oxygen with nonzero spin ($I = \frac{5}{2}$), occurs naturally in fractional abundance of only 3.7×10^{-4}. Although important NMR and ESR experiments involving [17]O have been performed, few observations have been made of [17]O nuclear quadrupole resonance (NQR) spectra in oxygen-containing substances. Quadrupole coupling constant data have been obtained from microwave spectra for gaseous, isotopically enriched SCO,[2] CO,[3] H_2O,[4] and H_2CO.[5] High-field NMR experiments have yielded quadrupole coupling constants in [17]O-enriched liquid water,[6] ice,[7] and chromium(III)-doped alumina.[8]

The double-resonance experiments pioneered by Redfield[9] and Hahn and co-workers[10,11] offer the possibility of very high sensitivity in observing pure quadrupole resonance spectra of any low-abundance spin system of half-integral spin $I \geq \frac{3}{2}$. Despite their wide potential application, these techniques have not thus far been widely employed. The few [17]O systems that have been studied by double-resonance methods include the isotopically enriched substances KH_2PO_4,[12] ice,[13a,b] and $BaClO_3\cdot H_2O$;[13c] NQR for natural abundance [17]O have been reported only for a series of eight organic solids,[11] and—using a slightly different technique—for two other organic compounds.[14] Most recently we have described several results from studies involving natural-abundance [17]O.[15]

Because oxygen is an important constituent of so many substances, particularly those of biological importance, a spectroscopic probe of the electronic environment about the oxygen nucleus would be of substantial and widespread utility. We have begun an extended series of studies of natural abundance level [17]O NQR spectra. The double-resonance experiment is adequately described elsewhere.[10,11,15,16] Briefly, it consists in cooling of the abundant I spin system (protons) by

adiabatic demagnetization in the laboratory frame, followed by application of high-level rf intended to excite the pure quadrupole transitions of a rare spin S system, [17]O. When the rf frequency is at or near resonance with an S spin quadrupole transition, thermal contact is established between the "hot" S spin system and cold I spin system. However, even though temperature equilibration may occur, the I spin temperature is changed very little because it has a much higher heat capacity than the S spin system. Repeated heating of the S spin system is effected by application of 180° phase shifts at intervals on the order of 500 μs. After about 10^4 such intervals, the spin temperature of the I system is substantially increased. The sample is returned to high magnetic field, and the I spin magnetization that remains is measured by applying a 90° pulse and sampling the free induction decay. The I spin system is then saturated and allowed to remagnetize for a given time, and the cycle is repeated at a new, incremented S channel frequency. The displayed spectra show the variation in I spin magnetization as a function of S channel frequency.

In this paper, we describe a few details of the experimental method employed, and present data for a series of carbonyl compounds, mainly organic in character. The [17]O data are interpreted in terms of the classic Townes–Dailey model; the results are compared with other structural and spectroscopic data for the compounds studied.

Description of the Spectrometer

A block diagram of the instrument, which is similar to that described by Slusher and Hahn,[10b] is shown in Figure 1. The proton (I channel) transmitter operates at about 40 MHz. A single coil design, consisting of a parallel resonant LC circuit, is employed. A short section of coaxial cable is used as a capacitor. The induction coil is tapped to effect impedance
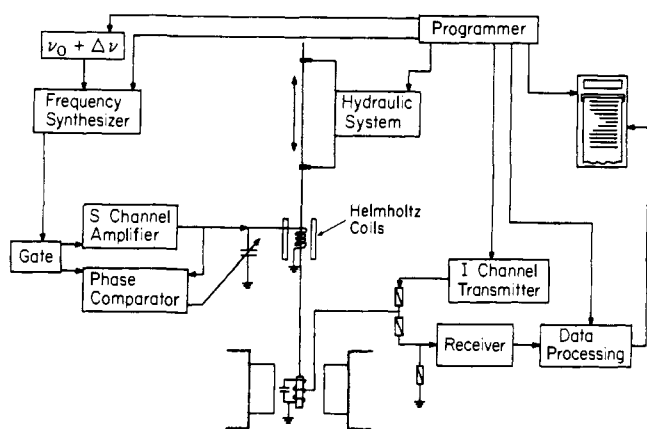
Figure 1. Block diagram of the NQR double resonance spectrometer.

Figure 2. Quadrupolar energy level diagram for nuclear spin $I = \frac{5}{2}$.

matching. The coil diameter is about 15 mm. An Arenberg Model PG-650C pulse oscillator is employed as rf source. A 90° pulse is about 5 μs long; overall receiver recovery time with a probe Q of about 60 is about 15 μs.

The S channel rf applied to the quadrupolar spin system is obtained from a digitally controlled PRD Model 7828 frequency synthesizer. It is amplified by a 20-W broad-band amplifier; the final output stage consists of a pair of 813 tubes. The output is fed to a tuned resonant circuit. To ensure a sufficiently large H_{1S}, it is necessary to maintain tuning of the sample tank circuit as the S channel frequency changes. The tuned circuit capacitance consists of several fixed-value high-voltage capacitors in parallel with a 500-pF air-variable capacitor. The fixed capacitors are automatically switched in or out of the circuit as the S channel frequency is swept. Fine tuning is effected by comparing the phase of the transmitter input signal with the output signal from the sample circuit. The air-variable capacitor is driven by a bidirectional shaded pole motor. The phase comparator is offset to compensate for phase shift within the transmitter itself. The transmitter is then tuned to obtain a zero phase shift within the comparator, corresponding to the absence of capacitive or inductive reactance in the output tuned circuit. This condition is precisely locatable, and was found to correspond accurately to maximum rf voltage across the coil. Using this tuning arrangement, it is possible to deliver high-amplitude rf to the sample circuit over the frequency range from about 180 kHz to 4 MHz, utilizing just one sample coil. Frequencies below 180 kHz are swept with a broad-band transmitter. A second coil provides access to the 4–8-MHz frequency region.

The timing of all phases of the experiment is controlled by a master digital programmer. After setting an initial S channel frequency, the increment by which the S channel frequency is advanced in each cycle, and the timing of all components of the experiment cycle, the instrument is capable of automatic scan over the entire frequency range accessible with a given sample coil.

Results

The [17]O nuclear spin transitions that we report are between energy levels determined by the quadrupole Hamiltonian, H_Q:[17]

$$H_Q = \frac{e^2 Q q_{zz}}{4I(2I-1)} \left[3I_z^2 - I^2 + \frac{\eta}{2}(I_+^2 + I_-^2) \right] \qquad (1)$$

The quantity $e^2 Q q_{zz}$ is the quadrupole coupling constant, η is the asymmetry parameter, and I is the nuclear spin. The field gradient tensor is diagonalized and the principal axis components chosen so that $|q_{ZZ}| \geq |q_{YY}| \geq |q_{XX}|$. The energy level
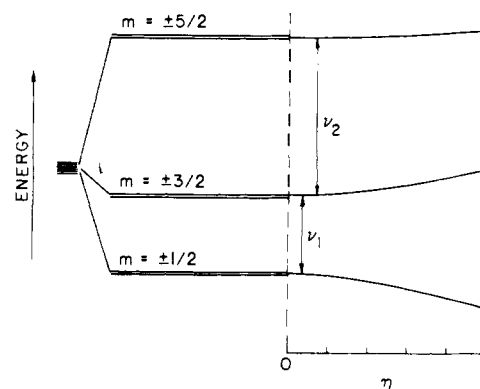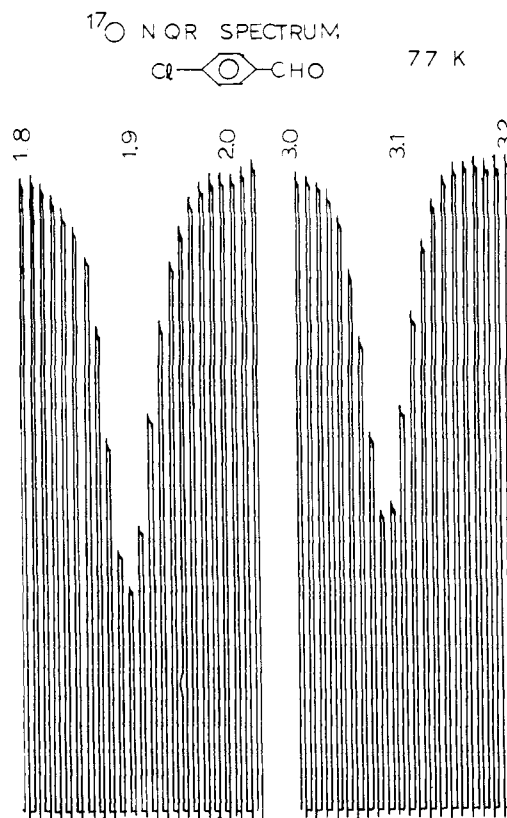

Figure 3. [17]O NQR double resonance spectrum of 4-chlorobenzaldehyde, with natural abundance [17]O (frequencies in megahertz).

diagram for $I = \frac{5}{2}$ as a function of η is shown in Figure 2. The two $\Delta m = 1$ transitions are the only ones allowed when $\eta = 0$. When η is about 0.4 or larger, the $\Delta m = 2$ transition acquires significant allowedness. Observation of the $|\pm\frac{5}{2}\rangle \leftrightarrow |\pm\frac{1}{2}\rangle$ transition can in some cases help resolve ambiguities in the interpretation of complex spectra.

The ratio of the $|\frac{5}{2}\rangle \leftrightarrow |\frac{3}{2}\rangle$ transition frequency, ν_2, to that of the $|\frac{3}{2}\rangle \leftrightarrow |\frac{1}{2}\rangle$, ν_1, varies smoothly from 2.0 for $\eta = 0$ to 1.0 for $\eta = 1$. The values of $e^2 Q q/h$ and η were calculated by interpolation in a table of relative transition energies obtained by finding the roots of the secular equation as a function of η.[18]

The [17]O NQR data for a series of carbonyl-containing compounds are listed in Table I. A typical [17]O spectrum, for 4-chlorobenzaldehyde, is shown in Figure 3. The two allowed transitions can be seen clearly at 3086 and 1900 kHz; ν_1 is normally more intense than ν_2, as in this example. With the exception of the two nitro compounds, there is just one oxygen

Table I. ^{17}O NQR Data at 77 K[a,b]

compd	$\nu_{5/2-3/2}$	$\nu_{3/2-1/2}$	e^2Qq/h	η
1. benzoyl fluoride	2494 (1)	1436 (1)	8.507 (2)	0.350 (1)
2. benzoyl chloride	2517 (2)	1477 (1)	8.613 (2)	0.376 (1)
3. 4-chlorobenzoyl chloride	2540 (3)	1522 (2)	8.723 (4)	0.403 (3)
4. 4-chlorobenzaldehyde	3086 (2)	1900 (1)	10.648 (2)	0.437 (2)
5. 4-nitrobenzaldehyde	3072 (3)	1910 (3)	10.618 (5)	0.449 (3)
6. 3-nitrobenz	3093 (3)	1929 (3)	10.697 (5)	0.453 (3)
7. benzoyl cyanide	3152 (2)	1902 (1)	10.838 (2)	0.412 (2)
8. 4,4′-dichlorobenzophenone	3175 (1)	1857 (1)	10.859 (2)	0.371 (1)
9. benzophenone	3183 (1)	1858 (1)	10.883 (2)	0.369 (1)
10. 4-chlorobenzophenone	3194 (1)	1867 (1)	10.923 (2)	0.370 (1)
11. benzoyl peroxide	*2596 (1)	1339 (1)	8.696 (2)	0.157 (3)
	3159 (2)	3126 (1)	11.916 (2)	0.987 (1)
12. benzyl chloroformate	*2350 (3)	1182 (1)	7.841 (3)	0.068 (1)
	2616 (2)	1628 (1)	9.044 (2)	0.450 (2)
13. potassium acid phthalate	1814 (1)	1498 (2)	6.608 (2)	0.775 (2)
	*2125 (5)	1294 (1)	7.318 (4)	0.423 (4)
14. phenyl benzoate	2627 (1)	1346 (1)	9.791 (1)	0.139 (4)
	*2755 (1)	1694 (1)	9.504 (2)	0.436 (1)
15. benzoic anhydride	2625 (2)	1361 (1)	8.801 (3)	0.170 (4)
	*2677 (2)	1569 (2)	9.159 (3)	0.374 (3)
	*2743 (2)	1658 (1)	9.435 (3)	0.414 (2)
16. phthalic anhydride	2238 (1)	1366 (1)	7.711 (1)	0.425 (2)
	*2655 (2)	1427 (1)	8.953 (2)	0.243 (2)
	*2655 (2)	1485 (1)	9.012 (2)	0.308 (2)
17. maleic anhydride	2138 (1)	1434 (1)	7.491 (1)	0.539 (1)
	*2743 (1)	1545 (2)	9.322 (3)	0.318 (2)
18. chloroacetic anhydride	2237 (1)	1175 (5)	7.515 (6)	0.199 (9)
	2452 (1)	1256 (2)	8.205 (3)	0.138 (6)
	*2715 (3)	1507 (1)	9.204 (3)	0.296 (3)
	*2715 (3)	1560 (1)	8.690 (2)	0.446 (2)
19. phthalimide	2642 (1)	1321 (1)	8.807 (3)	0.000 (1)
	*2818 (1)	1468 (1)	9.455 (2)	0.181 (2)
20. phthalide[c]	*2505 (2)	1256 (1)	8.354 (2)	0.046 (17)
	2552 (1)	1701 (1)	8.931 (1)	0.532 (1)
21. potassium bicarbonate	2232 (2)	1358 (2)	7.686 (3)	0.422 (3)
	*2050 (2)	1613 (2)	7.399 (3)	0.720 (4)
	1808 (2)	1715 (2)	6.765 (3)	0.934 (3)
22. sodium bicarbonate	2245 (5)	1310 (5)	7.675 (8)	0.368 (8)
	*2012 (2)	1705 (2)	7.366 (3)	0.804 (2)
	1822 (2)	1635 (5)	6.744 (5)	0.870 (5)
23. sodium formate	2113 (1)	1321 (1)	7.311 (2)	0.456 (2)

[a] Transition frequencies in units of kHz, e^2Qq/h in units of MHz. Uncertainties in the last place are indicated in parentheses. [b] Where more than one type of oxygen is present, the transitions assigned to carbonyl oxygen are denoted by an asterisk. [c] Phthalide = 1(3)-isobenzofuranone.

per molecule for the first ten compounds listed in Table I, and assignment of the spectrum is straightforward.[19] For compounds 9–12, a total of four transitions are observed, as expected. For benzoyl peroxide, benzyl chloroformate, and phenyl benzoate, only one set of pairings of the transitions is possible. In the case of potassium acid phthalate, the intensity pattern, and analogy to the other compounds studied, dictates the pairing assignment. The spectrum of this compound is shown in Figure 4. Note that the 1814- and 1498-kHz lines are sharp and intense, whereas the 2125- and 1294-kHz signals are broad and weak. It seems reasonable that the two signals due to a given ^{17}O should bear similar characteristics.[15] In agreement with this assignment, a weak absorption is seen at 3310 kHz; this signal is ascribed to the $|\pm^{5}/_{2}\rangle \leftrightarrow |\pm^{1}/_{2}\rangle$ transition of the spins that give rise to the 1814- and 1498-kHz pair of transitions.

The ^{17}O spectra for $KHCO_3$ and $NaHCO_3$ are complex; there are three crystallographically nonequivalent oxygens per unit cell,[20,21] leading to six $\Delta m = 1$ transitions. All six are observed. The assignments given in Table I are based in part on the similarities expected for line shapes of the two transitions assigned to a given oxygen, but most importantly on observations of all three $\Delta m = 2$ transitions. It is noteworthy that, although the ^{17}O NQR spectra for the two bicarbonate salts

are closely similar, $KHCO_3$ is reported to be dimeric in the solid,[20] whereas $NaHCO_3$ possesses a chain structure.[21] Other aspects of the spectra of these hydrogen-bonded systems are discussed in part 3 of this series. We are concerned here only with assigning the $C=O$ transitions.

The ^{17}O NQR spectrum for $KHCO_3$ is shown in Figure 5. Note that the pairs of related transitions differ considerably in width. The variation in line width is likely to be related to the rates of cross relaxation between the ^{1}H and ^{17}O spin systems during zero-field irradiation.[10b,15] In turn, the cross-relaxation rate, $1/T_{IS}$

$$1/T_{IS} = {}^{1}/_{2} \sin^2 \nu_S M_2{}^{IS} J(\Delta\omega_e) \qquad (2)$$

is proportional to $M_2{}^{IS}$, the contribution made by the particular set of S spins under irradiation to the second moment of the I spins, assuming 100% isotopic abundance. Equation 2 implies that the rate of change of proton spin temperature increases rapidly as the proton-^{17}O distance decreases. When the conditions of the experiment are such that the change in H spin magnetization is not effectively saturated in detecting the ^{17}O spins that undergo fastest cross relaxation, the total change in proton spin temperature will be largest upon irradiation of the oxygen atoms closest to the protons. Figure 6 shows the asymmetric unit in the crystal structure of $KHCO_3$.
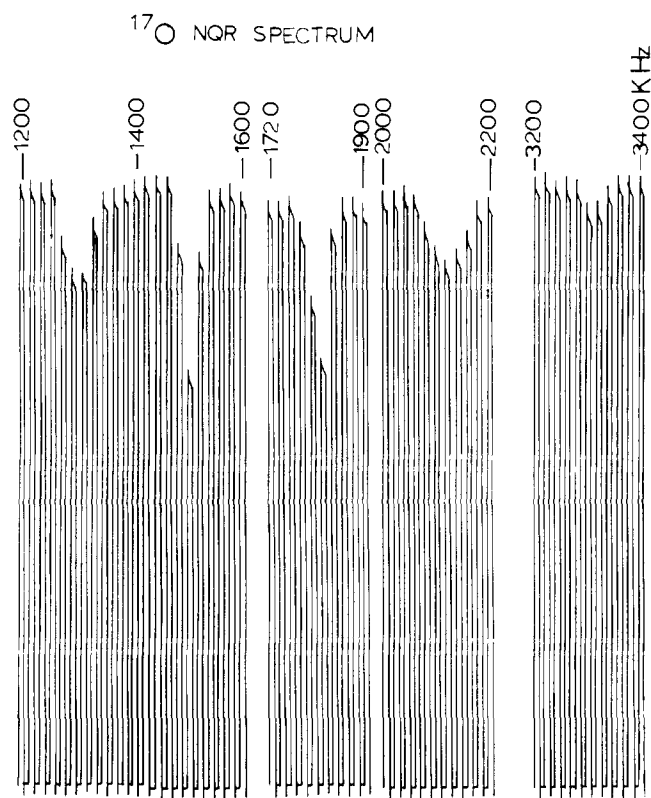
Figure 4. ^{17}O double resonance NQR spectrum of potassium acid phthalate.
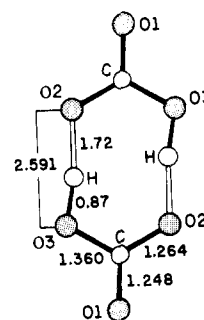

Figure 6. Asymmetric unit in the crystal structure of $KHCO_3$.[20] The bond distances shown were determined from data taken at 95 K.

completely, even when off resonance a bit, thus leading to a flattening in the minima.[22] On the basis of these considerations we assign the broadest and most intense pair of transitions at 2232 and 1358 kHz in the spectrum of Figure 5 to O_3, the pair at 1808 and 1715 kHz to O_2, and the pair at 2050 and 1613 kHz to O_1. On the basis of the crystal structure for $NaHCO_3$, it seems reasonable to assign the ^{17}O transitions in this compound by analogy to the $KHCO_3$ spectrum.

In the course of obtaining the ^{17}O NQR spectra, the ^{14}N NQR transitions in benzoyl cyanide were seen at 3339, 3043, and 296 kHz (e^2Qq_{zz} = 4256 kHz, η = 0.139);[39] K ($I = 3/2$) transitions were seen at 1011 ± 3 and 745 ± 3 kHz in potassium acid phthalate and $KHCO_3$, respectively; the ^{23}Na ($I = 3/2$) transition in $NaHCO_3$ was seen at 351 ± 1 kHz.

Application of the Townes–Dailey Model

Our purpose in this section is to outline a simple model for interpretation of the NQR data for singly connected oxygen, notably in organic carbonyl compounds. The analysis of ^{17}O NQR data for other bonding environments will be discussed in later papers.

The model put forth by Townes and Dailey[23] in the early years of NQR spectroscopy has continued to serve as the simplest and most useful framework for discussing NQR results for the lighter elements in covalent bonding environments. The field gradient tensor is assumed to arise from an imbalance

The distances from the two hydrogens in this unit to the oxygen atoms of adjacent units are sufficiently large that only the ^{17}O–H interactions of the asymmetric unit need be considered. It is evident from Figure 6 that the proton–^{17}O dipolar interaction, and thus $1/T_{IS}$, will vary in the order H-O_3 > H-O_2 > H-O_1.

The large variations in line width observed in the ^{17}O spectrum of $KHCO_3$ are the result of saturation effects; those ^{17}O spins closest to the protons can be expected to "saturate" most
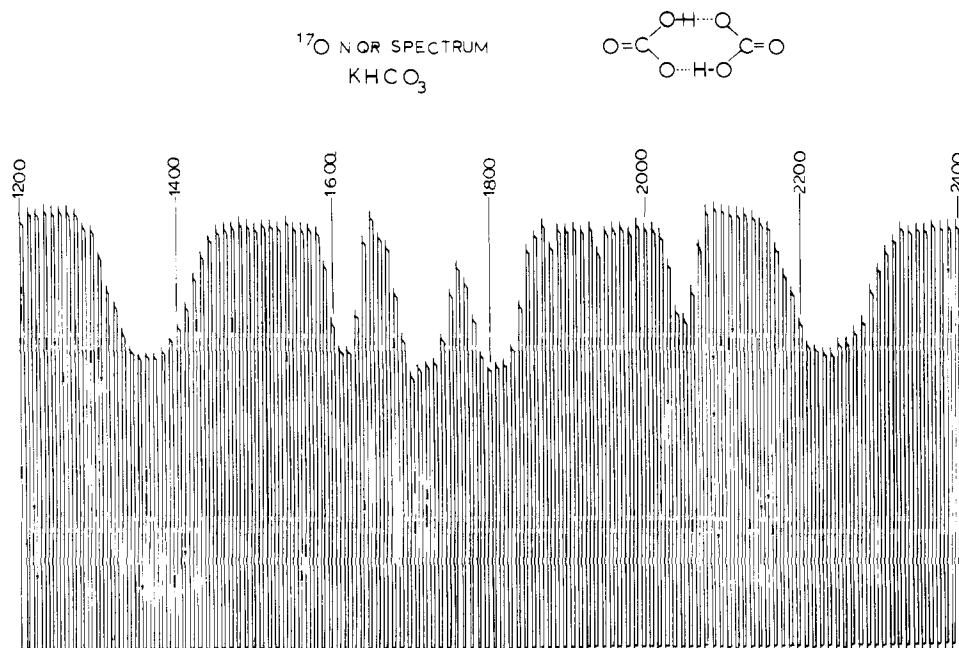

Figure 5. ^{17}O double resonance NQR spectrum of $KHCO_3$ (frequencies in kilohertz).

Table II. Analysis of Oxygen p Orbital Populations in 4-Chlorobenzaldehyde, Assuming 25% s Character in the Oxygen σ Orbital

case	rel magnitudes of tensor components[a]	sign of e^2Qq_{zz}/h	p_π	p_σ
1	$\|zz\| \geq \|yy\| \geq \|xx\|$	+	2.148	2.778
2	$\|zz\| \geq \|xx\| \geq \|yy\|$	+	1.852	2.580
3	$\|zz\| \geq \|yy\| \geq \|xx\|$	−	1.852	1.221
4	$\|zz\| \geq \|xx\| \geq \|yy\|$	−	2.148	1.420
5	$\|yy\| \geq \|xx\| \geq \|zz\|$	+	1.416	1.420
6	$\|yy\| \geq \|zz\| \geq \|xx\|$	+	1.565	1.221
7	$\|yy\| \geq \|xx\| \geq \|zz\|$	−	2.584	2.580
8	$\|yy\| \geq \|zz\| \geq \|xx\|$	−	2.435	2.778
9	$\|xx\| \geq \|yy\| \geq \|zz\|$	+	2.584	2.197
10	$\|xx\| \geq \|zz\| \geq \|yy\|$	+	2.435	1.803
11	$\|xx\| \geq \|yy\| \geq \|zz\|$	−	1.416	1.803
12	$\|xx\| \geq \|zz\| \geq \|yy\|$	−	1.565	2.197

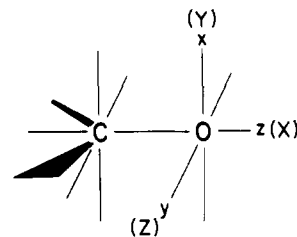[a] With reference to the *molecular* axis system, Figure 7.

Figure 7. Orientation of electric field gradient tensor axes in the molecular coordinate system of carbonyl compounds. The molecule-referenced axis system is shown as x, y, z. The field gradient tensor axes of formaldehyde[5] are labeled X, Y, Z, in accord with the convention $|V_{ZZ}| \geq |V_{YY}| \geq |V_{XX}|$ ($V = eq$).

in the populations of valence level p or d orbitals centered on the atom in question. For ^{17}O, only the 2p orbital populations are of relevance.

It is convenient to discuss the Townes–Dailey model in terms of the molecular axis system, x, y, z, oriented as shown in Figure 7. However, the axes of the field gradient tensor, denoted by X, Y, and Z, may be differently oriented, to remain consistent with the convention that $|q_{ZZ}| \geq |q_{YY}| \geq |q_{XX}|$ (vide infra).

The valence level atomic orbitals of oxygen, and associated orbital populations, appropriate to the oxygen of a carbonyl group can be written as follows:

orbital	orbital population
$\phi_1 = \upsilon_{2x}$	p_π
$\phi_2 = \upsilon_{2y}$	2
$\phi_3 = \alpha\upsilon_{2s} - \sqrt{1 - \alpha^2}\upsilon_{2z}$	p_σ
$\phi_4 = \sqrt{1 - \alpha^2}\upsilon_{2s} + \alpha\upsilon_{2z}$	2

$$(3)$$

υ_{2s}, υ_{2x}, υ_{2y}, and υ_{2z} are the oxygen 2s and 2p atomic orbitals, respectively; ϕ_2 and ϕ_4 represent the lone-pair orbitals, each containing two electrons. ϕ_1 is the π bond orbital with population p_π, and ϕ_3 is the σ bond orbital, with population p_σ. The quantity α^2 represents the fractional s character in the oxygen orbital used to form the σ bond. Because oxygen in the carbonyl group is singly connected, there are no experimental evidences such as bond angle data that might be employed to assign the hybridization of oxygen orbitals. Since υ_{2x} and υ_{2y} are both orthogonal to the C–O σ bond, only the derived p_σ population is affected by the value assumed for α^2.

Let q_{210} be the field gradient at the ^{17}O nucleus generated by a single electron in υ_{2z}. Then, according to the Townes–Dailey model, the major components of the field gradient tensor are expressible in terms of the orbital populations and fractional s character, as follows:

$$q_{zz} = \{-1 - p_\pi/2 + p_\sigma(1 - \alpha^2) + 2\alpha^2\}q_{210}$$

$$q_{yy} = \{2 - p_\pi/2 - p_\sigma(1 - \alpha^2)/2 - \alpha^2\}q_{210} \qquad (4)$$

$$q_{xx} = \{-1 + p_\pi - p_\sigma(1 - \alpha^2)/2 - \alpha^2\}q_{210}$$

The value for q_{210} can be determined from analysis of the hyperfine structure constant, b_2, in the spectra of atomic ^{17}O. In a paramagnetic resonance experiment Harvey determined that b_2 in the ^3P ground state of atomic ^{17}O is -10.438 ± 0.030 MHz.[24] This quantity is equal to $2e^2Q/5\langle r^3\rangle$; since $q_{210} = -\frac{4}{5}(e^2Q/\langle r^3\rangle)$, we have $e^2Qq_{210}/h = 20.9$ MHz.

The NQR experiment provides two observables, e^2Qq_{zz}/h and η. However, eq 4 contain three parameters, p_σ, p_π and α^2. The calculated value for p_π is independent of the choice of α^2,

whereas p_σ does depend on α^2. If we let $p_\sigma{}^0$ represent the orbital population when α^2 is zero, then

$$p_\sigma{}^0 = p_\sigma(1 - \alpha^2) + 2\alpha^2 \qquad (5)$$

The situation that obtains here is analogous to that for singly connected chlorine, in which the extent of s orbital participation in the σ bond has been debated.[25] Estimates of s character in the chlorine σ bond vary from zero to 15%. However, for nitrogen and oxygen a larger degree of s character in bonding σ orbitals is expected. In what follows we assume $\alpha^2 = 0.25$, somewhat less than the 0.33 which would be expected with a pure sp^2 hybridization of the σ and two lone pair orbitals. The effect on the derived orbital populations of varying the assumed value for α^2 is discussed later.

We do not know a priori either the sign of the quadrupole coupling constant or the relative values of q_{zz}, q_{yy}, and q_{xx}. There are in fact 12 possible combinations of eq 4. All of these 12 possible combinations, with the corresponding values for p_σ and p_π, are listed for chlorobenzaldehyde in Table II. It is evident that most of the combinations lead to physically unreasonable results, such as atomic orbital populations greater than 2. Of the four cases that remain, 3 and 11 lead to orbital populations in the vicinity of 1.8, suggestive of a highly polar σ bond and a low π bond order, with most of the charge resident on oxygen. Since this is at variance with the widely accepted and solidly established model of the carbonyl bond as consisting in substantial measure of both σ and π components, these two solutions can also be rejected. Cases 5 and 6 remain as viable possibilities. The choice between these two for 4-chlorobenzaldehyde can be made by reference to the field gradient tensor data obtained from the microwave spectrum of formaldehyde.[5] The field gradient tensor axes in that molecule are shown as parenthesized capital letters in Figure 7. The microwave data correspond to case 5 of Table II, with e^2Qq_{zz}/h positive. A Townes–Dailey analysis for formaldehyde based on the microwave data ($e^2Qq_{zz}/h = 12.37$ MHz, $\eta = 0.675$), assuming $\alpha^2 = 0.25$, yields $p_\sigma = 1.393$ and $p_\pi = 1.271$. These are quite reasonable values in relation to those listed for 4-chlorobenzaldehyde as case 5 of Table II. We therefore assume that for this and several other carbonyl compounds the principal axis system is the same as that derived for formaldehyde.

The carbonyl compounds listed in Table I can be grouped according to whether there is an atom on the carbonyl carbon, other than the carbonyl oxygen, with lone-pair electrons capable of π bond interaction with the carbon $2p_\pi$ orbital. In cases where such an interaction is possible, e^2Qq_{zz}/h is decidedly lower than for the other compounds. In these cases, one expects an increased value for the oxygen p_π. In valence bond terms, resonance structures of the form II contribute to the ground-state charge distribution.

Benzoyl chloride serves as a good illustration. In this compound, e^2Qq_{zz}/h for ^{35}Cl is 29.9 MHz.[26] This is to be compared
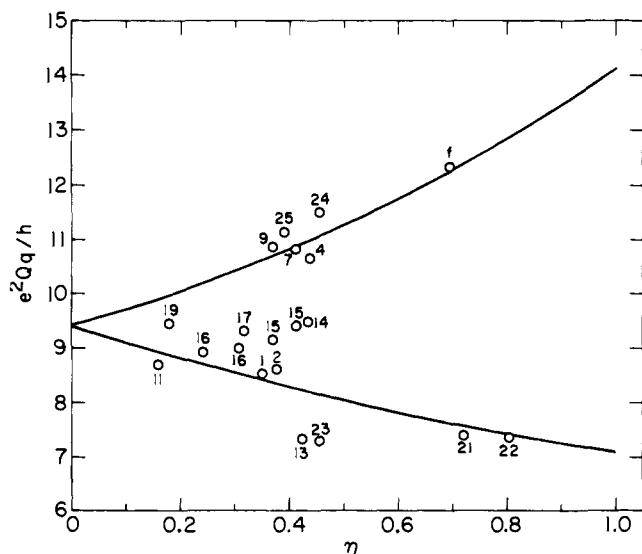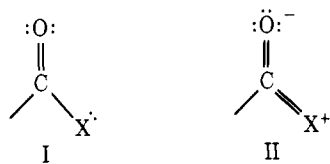
Figure 8. e^2Qq/h vs. η for a fixed assumed value of p_σ, s character = 25%. The line represents a calculated variation using the p_σ of gas-phase formaldehyde, 1.393, as reference. The numbered data points correspond to the numbering of Table I.

with 34.6 MHz for chlorobenzene,[27] in which Cl is also bonded to an sp^2-hybridized carbon atom. The lowered value in benzoyl chloride may be ascribed to π bonding as represented by structure II. One can roughly estimate from the ^{35}Cl NQR data that the C–Cl bond in benzoyl chloride contains at least 10% π-bond character. This π-bond interaction can be expected to result in a lowered π bond order between carbon and oxygen, with consequent increase in p_π.

It is generally recognized that in a multiple bond the π-electron distribution is more sensitive to structural variation than is the σ. This notion is supported by a set of SCF MO calculations for a set of related molecules carried out by Snyder and Basch.[31] For the four carbonyl derivatives shown in Table IV, the calculated oxygen $2p_\pi$ orbital population based on a Mulliken population analysis varies over a considerable range whereas the corresponding $2p_\sigma$ population is relatively invariant.

As a means of testing the assumption that p_σ is relatively invariant among the compounds studied, one can calculate e^2Qq/h and η as a function of varying p_π. A resulting graph of e^2Qq/h vs. η for the case where p_σ is held constant at 1.393 (the value calculated for formaldehyde) and $\alpha^2 = 0.25$ is shown in Figure 8. The quantity e^2Qq/h is largest for a small p_π; for example, e^2Qq/h is about 13 MHz, η about 0.8 for $p_\pi = 1.2$. In this regime $|q_{yy}| > |q_{xx}| > |q_{zz}|$. As p_π increases, both e^2Qq/h and η decrease. The asymmetry parameter is zero at the point $p_\pi = p_\sigma{}^0$. At still larger values for p_π, η again increases as e^2Qq/h continues to decrease. Thus, this simple model leads to the prediction that the q_{xx} and q_{zz} components of the field gradient tensor change in relative magnitude at e^2Qq/h about 9.4 MHz, corresponding to p_π about 1.55.

Figure 8 shows the NQR data of several compounds from Table I. The compounds chosen are those for which the assignment of the carbonyl resonances is certain or relatively unambiguous. The simple model matches the observed behavior reasonably well. On the basis of this agreement we

conclude that the presence of an atom containing nonbonding electron pairs on the carbonyl carbon ordinarily leads to a sufficient increase in p_π so that case 6 of Table II, $|q_{yy}| \geq |q_{zz}| \geq |q_{xx}|$, applies.

Having once decided on the relative values of q_{xx}, q_{yy}, and q_{zz}, and assuming a value for α^2, for a given compound, the observed values of e^2Qq/h and η can be converted into values for p_σ and p_π. It is not necessary to assume a fixed value for p_σ.

Table III shows the results of the population analysis carried out for all the carbonyl group data of Table I, as well as for a few data taken from Hsieh, Koo, and Hahn.[11] The applicable assumption regarding the relative magnitudes of field gradient tensor components is denoted in the column labeled "tensor", using the numbering of Table II. The p_σ populations are calculated for assumed values of α^2 of 0.25 and 0.15. The effect of an increased value for α^2 is to reduce p_σ, and thus to reduce the net charge on oxygen, Q_O, given by $2 - (p_\pi + p_\sigma)$.

It should be noted that phthalimide represents the one case among the compounds of Table I in which a carbonyl group is perturbed by a hydrogen-bonding interaction.[15] The carbonyl data asterisked in Table I and included in Table III correspond to the carbonyl group not involved in hydrogen bonding.

Discussion

The ^{17}O NQR results presented here are the first extensive set of data pertaining to oxygen in a particular functional group. They show that the ^{17}O NQR data are sensitive to the details of the chemical environment, and thus that ^{17}O NQR spectroscopy might be useful as a structural probe.

In some cases splittings due to crystallographic nonequivalencies of structurally equivalent oxygens are seen. Such nonequivalencies are commonly observed in the NQR spectra of halogens, and—less obviously—in ^{14}N spectra. Comparisons with known crystal structures are often useful, but limited by the fact that the NQR data are obtained at 77 K, whereas the X-ray structural results ordinarily pertain to room temperature.

The NQR data provide information about the components of the electric field gradient at the nucleus in question. These field gradient components are the expectation values of one-electron operators, and are thus a reflection of the ground-state charge distribution. Correlation with other physical and chemical properties of the molecules in question should thus depend on the extent to which these other properties are dependent on, or can be related to, the ground-state charge distribution. Unfortunately, there are not many other such properties in addition to field gradient data. Bond stretching force constants are not, although reasonably good relationships between bond order and force constant have been demonstrated in select cases. Carbon–oxygen bond stretching force constant data are not available for the compounds of Table III. The C=O group frequency relates only crudely to the force constant, because other motions of the molecular framework contribute in varying degrees to the normal mode. As a result of these complications, it does not seem possible to discern any useful relationship between the ^{17}O NQR data and observed C=O groups stretching frequencies in these carbonyl compounds.

It might be expected that the chemical shift of the ^{17}O NMR signal for the compounds in solution would reflect the total net charge on the atom, as with relationships worked out for ^{13}C chemical shifts.[28] However, detailed comparisons of ^{17}O NQR data with ^{17}O NMR chemical shift data must wait upon more extensive data. Nevertheless, what is presently known suggests that there should be a reasonably good correlation between the ^{17}O chemical shift in carbonyl groups and the π bond order as reflected in the values of p_π derived from the NQR data.[29,30]

Table III. Population Analysis of Carbonyl Oxygen Orbitals

	compd	e^2Qq/h^a	η	tensor[b]	p_π	p_σ $\alpha^2 = 0.15$	$\alpha^2 = 0.25$	$-Q_O{}^c$
1.	benzoyl fluoride	8.507	0.350	6	1.640	1.465	1.393	1.03
2.	benzoyl chloride	8.613	0.376	6	1.639	1.454	1.381	1.02
3.	4-chlorobenzoyl chloride	8.723	0.403	6	1.639	1.442	1.368	1.01
4.	4-chlorobenzaldehyde	10.648	0.437	5	1.416	1.488	1.420	0.84
5.	4-nitrobenzaldehyde	10.62	0.449	5	1.416	1.492	1.424	0.84
6.	3-nitrobenzaldehyde	10.7	0.452	5	1.411	1.488	1.420	0.83
7.	benzoyl cyanide	10.838	0.412	5	1.410	1.474	1.403	0.81
8.	4,4'-dichlorobenzophenone	10.859	0.371	5	1.416	1.464	1.393	0.81
9.	benzophenone	10.883	0.369	5	1.415	1.463	1.391	0.81
10.	4-chlorobenzophenone	10.923	0.370	5	1.413	1.461	1.389	0.80
11.	benzoyl peroxide	8.696	0.157	6	1.606	1.485	1.416	1.02
12.	benzyl chloroformate	7.841	0.068	6	1.632	1.414	1.336	0.97
13.	potassium acid phthalate	7.318	0.423	6	1.700	1.529	1.467	1.17
14.	phenyl benzoate	9.504	0.436	6	1.611	1.387	1.306	0.92
15.	benzoic anhydride	9.159	0.374	6	1.616	1.420	1.343	0.96
		9.435	0.414	6	1.611	1.395	1.315	0.93
16.	phthalic anhydride	8.953	0.243	6	1.606	1.455	1.382	0.99
		9.012	0.308	6	1.613	1.440	1.366	0.98
17.	maleic anhydride	9.322	0.318	6	1.601	1.419	1.342	0.94
18.	chloroacetic anhydride	9.204	0.296	6	1.603	1.431	1.355	0.96
		8.690	0.446	6	1.646	1.438	1.363	1.01
19.	phthalimide	9.455	0.181	6	1.575	1.435	1.360	0.94
20.	phthalide	8.354	0.046	6	1.606	1.522	1.459	1.06
21.	potassium bicarbonate	7.399	0.720	6	1.731	1.483	1.415	1.15
22.	sodium bicarbonate	7.366	0.804	6	1.742	1.474	1.404	1.15
23.	sodium formate	7.311	0.456	6	1.703	1.526	1.463	1.17
24.	*p*-benzoquinone[d]	11.511	0.454	5	1.366	1.450	1.377	0.74
25.	1,5-dichloroanthraquinone[d]	11.139	0.392	5	1.397	1.455	1.382	0.78

^{a} MHz. ^{b} See Table II. ^{c} Formal charge on oxygen, assuming $\alpha^2 = 0.25$. ^{d} Data from ref 11.

Table IV. Comparison of Calculated and Observed Field Gradient Quantities

results from SCF MO calculations[31]	O‖HCH	O‖HCF	O‖HCOH	HC⟨O⁻⟩⟨O⟩
p_π	1.292	1.351	1.434	1.621
p_σ	1.313	1.245	1.251	1.318
Q_O	0.31	0.28	0.38	0.62
σ overlap pop.	0.584	0.763	0.773	0.398
π overlap pop.	0.433	0.417	0.393	0.264
$eq_{yy}{}^a$ (V_{ZZ})	−2.612	−2.210	−2.061	−1.742
eq_{xx}	1.916	1.425	1.093	0.420
eq_{zz}	0.697	0.786	0.968	1.322
e^2Qq/h, MHz	16.2	13.8	12.8	10.5
η	0.47	0.28	0.06	0.51

exptl results	O‖4-ClC₆H₄CH	O‖C₆H₅CF	O‖C₆H₅COC₆H₅	HC⟨O⁻⟩⟨O⟩
e^2Qq/h, MHz	10.65	8.51	9.50	7.34
η	0.44	0.35	0.44	0.45
$Q_O{}^b$	0.84	1.03	0.92	1.17

^{a} The labels *xx*, *yy*, *zz* refer to the diagonalized field gradient tensor in the molecule-based coordinate system, Figure 7. The field gradient tensor axes are labeled in accordance with the convention $|V_{ZZ}| \geq |V_{YY}| \geq |V_{XX}|$. ^{b} Net charge on oxygen based on the Townes–Dailey analysis, Table II.

In general, a small value for p_π, which connotes a high degree of C–O π bond order, should correspond to the largest upfield chemical shifts. Thus aldehydes and ketones, $p_\pi \sim 1.4$, fall in the 550–600-ppm range, upfield from H_2O; esters and acyl halides, $p_\pi \sim 1.6$, in the 350–500 ppm range; carboxylates, $p_\pi \sim 1.7$, in the vicinity of 200 ppm.

As a means of evaluating some of the assumptions made in setting up the model we have used, it is useful to consider the results of molecular orbital calculations. The molecules we have examined are, in general, too large to admit of reasonably thorough SCF molecular orbital calculations. However, Synder and Basch have provided the results of an extensive set of SCF molecular orbital calculations,[31] some of which are germane to the present work. Table IV shows the results of their calculations for a series of four molecules which form a more or less parallel series for comparison with four compounds from Table I, also shown in Table IV. The four model compounds of Table I are listed in the order of decreasing values of eq_{yy}, which is the major axis component of the field gradient tensor in all cases. (Recall that the *x*, *y*, *z* coordinate system is oriented with respect to the C–O bond axis, Figure 7.) This is also the order of increasing p_π, the population of the π oxygen 2p orbital. There is comparatively little change in the analogous σ orbital population, p_σ, in this same series. (However, the σ overlap populations do vary considerably throughout the series.)

Basch and Snyder have tabulated the calculated values for the components of the electric field gradient tensor in the molecular coordinate system. From these, by a linear transformation in the molecular plane, the components of the diagonalized field gradient tensor can be obtained. The axes of the diagonalized tensor lie in every case within a degree or so of the *y* and *z* axes illustrated in Figure 7. We thus do not distinguish the axes of the diagonalized tensor from the *y* and *z* axes illustrated.

The largest component of the tensor, eq_{yy}, lies in the molecular plane and normal to the C–O bond axis. Thus, in the usual notation for field gradient tensors, this is denoted V_{ZZ}. From this quantity, using a value of Q for ^{17}O of -0.0265×10^{-24} cm²,[24] the values listed for e^2Qq/h ($e^2Qq/h = eQV_{ZZ}$) were calculated. Values for η are obtained from the expression $\eta = (V_{XX} - V_{YY})/V_{ZZ}$.

It is instructive to compare these calculated quantities with those experimentally determined for closely related substances, as listed in Table IV. The calculated results for the formyl compounds are not strictly comparable with those of the phenyl derivatives. However, the inductive properties of the phenyl group and hydrogen are closely similar. Although the phenyl group is capable of π interaction with the C=O group, the effect should not be large, and should be more or less constant throughout the series. Note, for example, that the ^{17}O NQR parameters are quite similar for 4-chlorobenzaldehyde and 4-chlorobenzophenone. Thus, the trends in calculated quantities should correspond reasonably well with corresponding changes in the series of analogous phenyl compounds. (It should be noted that phenyl benzoate was employed for the comparison with the formic acid calculations rather than formic acid itself, because formic acid is strongly hydrogen bonded in the solid. The ^{17}O NQR spectrum of formic acid is discussed in a later paper.)

The quadrupole coupling constants calculated from the full basis set of wave functions, with exact evaluation of the one-electron operator, are higher than those observed experimentally. However, no correction has been applied for Sternheimer effects,[32] nor has any allowance been made for the fact that the experimental data are obtained on solids. Both effects would contribute to a lowered quadrupole coupling constant. More importantly, the trend in values of e^2Qq/h is in rough agreement with experiment. Although HC(O)F and HC(O)OH are reversed, the presence of a substituent on the carbonyl carbon capable of π-bond interaction with carbonyl causes a lowering in the calculated quadrupole coupling constant. Similarly, the calculated value of e^2Qq/h is lowered still further by the presence of a negative charge, as in formate ion. The variation in η based on the calculated field gradient tensor components is of special interest. As the p_π population on oxygen increases, the relative values of the tensor components change; eq_{zz} grows relative to eq_{xx}. As a result η decreases, passes through zero, and again increases. In formate ion, with a relatively large value for η, the orientations of V_{YY} and V_{XX} are reversed with respect to formaldehyde. It is thus reasonable that for some carbonyl groups with environments intermediate between these extremes, e.g., benzoyl peroxide, benzyl chloroformate, and phthalimide, η might have relatively small values. The assignments made in Table I were based in part on these considerations.

In applying the Townes–Dailey analysis to the carbonyl ^{17}O data, we assumed that, when a group with lone-pair electrons capable of π interaction is bound to carbonyl, the increase in population of the oxygen p_π orbital is sufficient to cause a reversal in the relative values of eq_{xx} and eq_{zz}. Thus, for example, it was assumed in deriving the populations of Table III for benzoyl fluoride that $eq_{zz} > eq_{xx}$. In this respect the Townes–Dailey model does not yield agreement with the SCF calculations; in the latter the reversal in relative values of eq_{zz} and eq_{xx} occurs only when the oxygen p_π orbital population is increased considerably by the presence of negative charge in the carbonyl group. Despite the lack of agreement noted, the assumption in applying the Townes–Dailey model that case 6 ($eq_{zz} > eq_{xx}$) applies to benzoyl fluoride and related compounds seems the better choice for the present, especially in light of the empirical relationship observed in Figure 8. The alternative assumption results in variations in p_σ among the compounds studied, rather than in p_π.

The Townes–Dailey analysis of the experimental results leads to characteristically large charges Q_O on the atoms, in-

dependent of the assumption made regarding the relative values of eq_{xx} and eq_{zz}. These charges do not compare well with the much smaller charges based on a Mulliken population analysis of the SCF functions, Table IV. With the exception of benzoyl fluoride the overall variation in Q_O is reproduced. The relatively large value obtained for the fluoride is disturbing. It would appear that the charge distributions in the carbonyl group based on the Townes–Dailey model for ^{17}O NQR data should be treated with reservation until more extensive data are available for analysis.

In summary, the present work has shown that the ^{17}O NQR spectra of carbonyl groups are sensitive to chemical and crystalline environment. The value of ^{17}O NQR spectroscopy for structural diagnosis can be expected to increase as the number and variety of compounds studied increases. The NQR data provide interesting and interpretable information regarding charge distribution in the carbonyl group. However, detailed interpretations must await more extensive theoretical work, and correlations of the NQR data with other spectroscopic data, such as ^{17}O NMR chemical shifts, electronic spectra, ESCA, and so forth. In future papers we intend to report the NQR spectra for ^{17}O in a variety of other functional group environments.

References and Notes

(1) This research is supported by the National Institutes of Health, Institute of General Medicine, through Research Grant GM-23395.
(2) S. Geschwind, R. Gunther-Mohr, and J. Silvey, *Phys. Rev.*, **85**, 474 (1952).
(3) R. Rosenblum and A. H. Nethercot, *J. Chem. Phys.*, **27**, 828 (1957).
(4) M. J. Stevenson and C. H. Townes, *Phys. Rev.*, **107**, 635 (1957).
(5) W. H. Flygare and J. T. Lowe, *J. Chem. Phys.*, **43**, 3654 (1965).
(6) H. A. Christ and P. Diehl, *Proc. Colloq. AMPERE*, 224 (1962); (b) B. B. Garrett, A. B. Denison, and S. W. Rabideau, *J. Phys. Chem.*, **71**, 2606 (1967).
(7) H. W. Spiess, B. B. Garrett, R. K. Sheline, and S. W. Rabideau, *J. Chem. Phys.*, **51**, 1201 (1969).
(8) E. Brun, B. Derighetti, E. E. Hundt, and H. H. Nibuhr, *Phys. Lett. A*, **31**, 416 (1970).
(9) A. G. Redfield, *Phys. Rev.*, **130**, 589 (1963).
(10) (a) R. E. Slusher and E. L. Hahn, *Phys. Rev. Lett.*, **12**, C508 (1964); (b) R. E. Slusher and E. L. Hahn, *Phys. Rev.*, **166**, 332 (1968).
(11) Y. Hsieh, J. C. Koo, and E. L. Hahn, *Chem. Phys. Lett.*, **13**, 563 (1972).
(12) R. Blinc, J. Seliger, R. Osredkar, and A. Prelesnik, *Chem. Phys. Lett.*, **23**, 486 (1973).
(13) (a) D. T. Edmonds and A. Zussman, *Phys. Lett. A*, **41**, 167 (1972); (b) D. T. Edmonds, S. D. Garen, A. L. Mackay, A. A. L. White, and W. F. Sherman, *J. Magn. Reson.*, **23**, 505 (1976); (c) M. Shopover and A. M. Achlama, *J. Chem. Phys.*, **65**, 3657 (1976).
(14) R. Kado, Y. Takarada, and H. Halanaka, *Phys. Lett. A*, **47**, 49 (1974).
(15) T. L. Brown and C. P. Cheng, *Faraday Symp. Chem. Soc.*, in press.
(16) D. T. Edmonds, *Phys. Rep.*, **29**, 233 (1977).
(17) C. P. Slichter, "Principles of Magnetic Resonance", 2nd ed., Springer-Verlag, New York, 1978, p 287.
(18) T. P. Das and E. L. Hahn, "Nuclear Quadrupole Resonance Spectroscopy", Academic Press, New York, 1958, p 13.
(19) The ^{17}O NQR spectra of nitro groups have been unambiguously assigned from other experiments to be reported on later.
(20) J. O. Thomas, R. Tellgren, and I. Olovsson, *Acta Crystallogr., Sect. B*, **30**, 1155 (1974).
(21) W. H. Zachariasen, *J. Chem. Phys.*, **1**, 634 (1933).
(22) The result of a systematic investigation of the effects of variations in experimental parameters on line shape in ^{17}O spectra is the subject of a following paper in this series.
(23) C. H. Townes and B. P. Dailey, *J. Chem. Phys.*, **17**, 782 (1949).
(24) J. S. M. Harvey, *Proc. R. Soc. London, Ser. A*, **285**, 581 (1965).
(25) E. A. C. Lucken, "Nuclear Quadrupole Coupling Constants", Academic Press, New York, 1969, Chapter 7.
(26) P. J. Bray, *J. Chem. Phys.*, **23**, 703 (1955).
(27) H. O. Hooper and P. J. Bray, *J. Chem. Phys.*, **33**, 334 (1960).
(28) (a) J. B. Stothers, "Carbon-13 NMR Spectroscopy", Academic Press, New York, 1972; (b) G. J. Martin, M. L. Martin, and S. Ochet, *Org. Magn. Reson.*, **7**, 2 (1975).
(29) W. G. Klemperer, *Angew. Chem., Int. Ed. Engl.*, **17**, 246 (1978).
(30) C. Delseth and J.-P. Kintzinger, *Helv. Chim. Acta*, **59**, 466 (1976).
(31) L. C. Synder and H. Basch, "Molecular Wave Functions and Properties", Wiley-Interscience, New York, 1972.
(32) Reference 25, Chapter 5.